ACS POLYMERS Au
AN OPEN ACCESS JOURNAL OF THE AMERICAN CHEMICAL SOCIETY

pubs.acs.org/polymerau
Letter

Surface-Initiated PET-RAFT via the Z-Group Approach

Published as part of ACS Polymers Au virtual special issue "2023 Rising Stars".

Sai Dileep Kumar Seera and Christian W. Pester*

Cite This: *ACS Polym. Au* 2023, 3, 428–436
Read Online

ACCESS | Metrics & More | Article Recommendations | Supporting Information

ABSTRACT: Surface-initiated reversible addition–fragmentation chain transfer (SI-RAFT) is a user-friendly and versatile approach for polymer brush engineering. For SI-RAFT, synthetic strategies follow either surface-anchoring of radical initiators (e.g., azo compounds) or anchoring RAFT chain transfer agents (CTAs) onto a substrate. The latter can be performed via the R-group or Z-group of the CTA, with the previous scientific focus in literature skewed heavily toward work on the R-group approach. This contribution investigates the alternative: a Z-group approach toward light-mediated SI photoinduced electron transfer RAFT (SI-PET-RAFT) polymerization. An appropriate RAFT CTA is synthesized, immobilized onto SiO_2, and its ability to control the growth (and chain extension) of polymer brushes in both organic and aqueous environments is investigated with different acrylamide and methacrylate monomers. O_2 tolerance allows Z-group SI-PET-RAFT to be performed under ambient conditions, and patterning surfaces through photolithography is illustrated. Polymer brushes are characterized via X-ray photoelectron spectroscopy (XPS), ellipsometry, and water contact angle measurements. An examination of polymer brush grafting density showed variation from 0.01 to 0.16 chains nm^{-2}. Notably, in contrast to the R-group SI-RAFT approach, this chemical approach allows the growth of intermittent layers of polymer brushes underneath the top layer without changing the properties of the outermost surface.

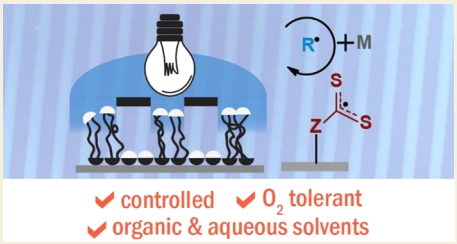

KEYWORDS: *polymer brushes, surface modification, light-mediated polymerization, controlled radical polymerization, RAFT polymerization*

1. INTRODUCTION

Modifying the surfaces of materials with polymers is significant to many fields, from microelectronics[1] to biotechnology[2] to nanocomposites.[3] To address the limitations of physiosorbed coatings (such as weak adhesion, sensitivity to environmental conditions, and limited long-term stability),[4] covalently surface-tethered polymer brushes provide a robust alternative.[5−7] Polymer brushes have shown promise for applications in various fields, including, but not limited to, stimuli-responsive surfaces,[8−10] drug delivery,[11] antifouling surfaces,[12−14] electronic materials,[15−17] catalysis,[18−23] and biosensing.[24−27]

A wide range of surface-initiated polymerization techniques exist to allow surface modification with polymer brushes.[7,28,29] In recent years, significant advances have been made in surface-initiated reversible-deactivation radical polymerization (SI-RDRP) and external control thereof.[30−32] SI-RDRP can be performed in ambient conditions, with tolerance to oxygen[33−37] and externally regulated (patterned) under mild visible wavelengths.[38,39] The preservation of functional chain ends affords uniform thicknesses and the ability to synthesize complex architectures (e.g., layered multiblock copolymer brushes) through techniques such as SI atom transfer radical polymerization (SI-ATRP),[40,41] SI reversible addition–fragmentation chain transfer polymerization (SI-RAFT),[42] SI nitroxide mediated polymerization (SI-NMP),[43] and others.[44,45]

For SI-RAFT, various distinct strategies exist. One approach follows surface-anchoring of radical initiators (e.g., azo compounds or peroxides) and addition of free chain transfer agent (CTA) to the reaction solution to cap the surface-tethered radical chain ends.[46,47] The alternative is anchoring the RAFT CTA itself onto the substrate, via either the R-[48−50] or the Z-group[51−56] (see Figure 1a).

For the R-group approach, the CTA is anchored through its leaving and reinitiating group. This approach behaves similarly to other "*grafting from*" approaches; the propagating radicals are present at the terminal end of the polymer chain, allowing synthesis of polymer brushes with high grafting density. Recently, our group[57] and Hawker and co-workers[58] reported on a light-mediated R-group approach: SI photoinduced electron transfer (PET) RAFT. SI-PET-RAFT provides good spatial control over surface patterning,[59] O_2 tolerance, operates

Received: September 15, 2023
Revised: November 9, 2023
Accepted: November 14, 2023
Published: November 20, 2023

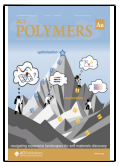

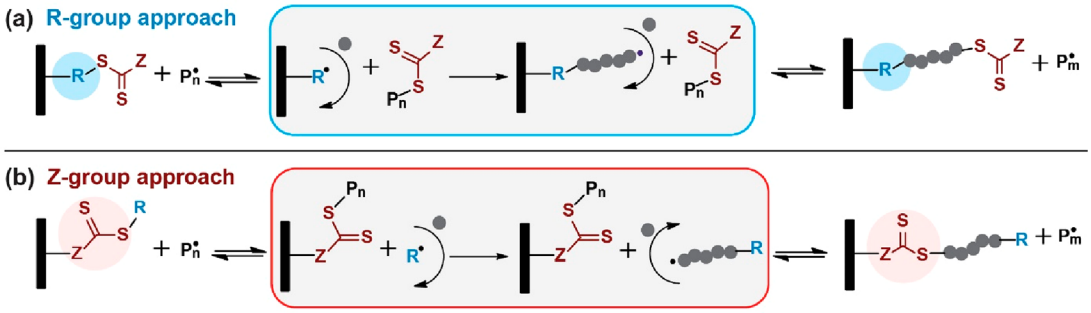

Figure 1. Schematic illustration of the resulting SI-RAFT polymerization mechanisms upon surface-immobilizing chain transfer agents (CTAs) via (a) the R-group and (b) the Z-group approach.

in both organic[60] and aqueous environments,[61] and can be used to modify organic substrates.[62] However, in grafting from approaches, the molecular weight distribution of polymer chains can be broadened due to bimolecular chain termination. The recombination of polymer chains is attributed to the fast migration of radicals on the surface through sequential chain-transfer reactions.[63]

In contrast, when the Z-group approach is used, the RAFT CTA remains tethered to the surface throughout the polymerization process (see Figure 1b). The reaction between the propagating radicals and the RAFT CTA occurs near the substrate surface. Mechanistically, achieving high-density grafted polymers using the Z-group approach can be challenging due to steric hindrance caused by the nearby attached polymer chains.[53,55,56] Because the propagation of chains occurs only in the solution, an advantage of the Z-group approach is the reduced bimolecular termination of growing polymer chains at the surface. This has been shown to lead to a narrower molecular weight distribution (dispersity) of the grafted polymer chains.[53,55,56]

Here, we investigate a Z-group approach towards light-mediated SI-PET-RAFT polymerization. We synthesized an appropriate RAFT CTA, immobilized it onto SiO_2, and explored the ability to control the growth (and chain extension) of polymer brushes in both organic and aqueous environments. We established the O_2 tolerance and the capability to pattern surfaces through photolithography. In contrast to the R-group SI-PET-RAFT approach, this chemistry allows the growth of intermittent layers of polymer brushes underneath the top layer without changing the properties of the outermost surface. We studied the resulting surfaces through X-ray photoelectron spectroscopy (XPS) to gather information about the chemical composition of the polymer brushes, while variable angle spectroscopic ellipsometry (VASE) was used to determine the final thicknesses, polymerization kinetics, and grafting densities of the polymer brush films. Water contact angle (WCA) measurements were conducted to assess the wettability of the surfaces, and optical microscopy enabled visual characterization of surface patterning.

2. RESULTS AND DISCUSSION

2.1. Synthesis of RAFT CTA and Functionalization of Substrates

Synthesis of the RAFT CTA for this work was inspired by previous work.[55] 3-(Mercaptopropyl) triethoxysilane and ethyl α-bromophenylacetate were used to synthesize the RAFT CTA for surface-initiated Z-group SI-PET-RAFT (see experimental information and Figure S1). Proton nuclear magnetic resonance spectroscopy (^{1}H NMR) confirmed the successful synthesis of the target compound. Immobilization onto substrates was performed following an established procedure (see experimental information and Figure S2).[57] X-ray photoelectron spectroscopy (XPS) confirmed the covalent attachment of the RAFT CTA onto SiO_x wafers via the presence of S 2s and S 2p at $BE_{S\ 2s}$ = 230 eV and $BE_{S\ 2p}$ = 164 eV, respectively, in the photoelectron spectrum (see Figures 2b and S3).

2.2. Influence of Monomer to Solvent Concentration on the Brush Growth, Grafting Density Studies

SI-PET-RAFT polymerization kinetic studies were performed using inhibitor free *N,N*-dimethylacrylamide (DMA) as the monomer and zinc tetraphenylporphyrin (ZnTPP) as the photocatalyst (PC). Blue light with a wavelength of λ = 405 nm, (intensity = 2400 lx) was chosen for irradiation as it aligns with the absorption region of ZnTPP. The ratio of DMA to ZnTPP was fixed at [M]:[PC] = 500:0.025 based on our previous R-group SI-PET-RAFT study.[57] Three different monomer concentrations (3.7, 15, and 30 mol/L) were studied. Brush thickness increased with irradiation time for all three concentrations (see Figure S4) as determined by variable angle spectroscopic ellipsometry (VASE). XPS was used to confirm the presence of the DMA-specific nitrogen N 1s peak at $BE_{N\ 1s}$ = 400 eV in the survey spectrum (see Figure 2b), while the high-resolution carbon C 1s spectrum showed the DMA-specific ratios of C═O:C−N:C−C = 1:2.1:1.9 (theoretical ratio 1:2:2; see Figure S3b).

Previous reports on PET-RAFT[64] and SI-PET-RAFT[57] via the R-group approach describe how oxygen can be scavenged by dimethyl sulfoxide (DMSO) in the presence of ZnTPP. To probe this for the Z-group approach, experiments were also conducted in ambient conditions (i.e., presence of oxygen). Figure 2c shows that polymer brush growth rates in ambient conditions, dd/dt = 5.5 nm h^{-1} fully open to air, were similar to inert conditions (dd/dt = 5.4 nm h^{-1} in nitrogen atmosphere). Hence, the described process requires no rigorous degassing of the solution mixture prior to polymerization.

Control experiments were conducted to confirm that the polymer brushes were indeed covalently attached to the surface and not merely physiosorbed. No polymer growth occurred on bare unfunctionalized Si wafers, in the dark, or in the absence of photocatalyst. This indicated that the observed thicknesses are from polymer brushes rather than adsorbed polymers grown in solution and that polymerization does not occur without the PC. In one of the experiments, the initiator layer

https://doi.org/10.1021/acspolymersau.3c00028
ACS Polym. Au 2023, 3, 428−436

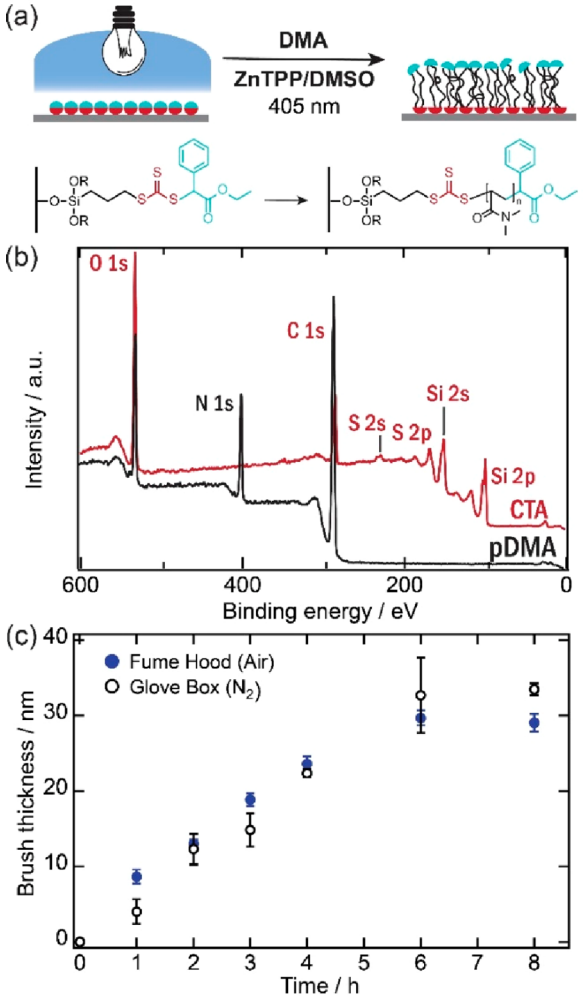

Figure 2. (a) Schematic of surface-initiated photoinduced electron transfer-reversible addition−fragmentation chain transfer polymerization (SI-PET-RAFT) via Z-group approach. (b) X-ray photoelectron spectroscopy (XPS) of survey spectra for RAFT CTA and p(DMA) polymer brush. (c) Polymer brush thickness vs irradiation time of DMA using ZnTPP as a photocatalyst, under (λ = 405 nm) wavelength light, both in an inert nitrogen atmosphere (open circle) and in open to air conditions (filled circle).

on the Si wafers was degraded by shining a UV-light (λ = 365 nm) through a photomask for 16 h. The wafer was rinsed thoroughly, and the polymerization of DMA was attempted. The micrograph (see Figure S5) confirmed patterning on the wafer and no polymer brush growth in the regions that were previously exposed to UV light.

At $[M]_0$ = 3.7 mol/L, the polymer brush growth rate was determined as dd/dt = 2.8 nm h^{-1}. To study the influence of monomer concentration on polymer brush growth, the concentration was increased to 15 mol/L. As expected, based on kinetic descriptions of RDRP, this higher monomer concentration led to an increase in polymerization rate to 5.4 nm h^{-1}. As the rate of polymerization in solution increases, so will the molecular weight of the polymer chain and the thickness of the polymer brush. However, upon further increasing the monomer concentration to [M] = 30 mol/L, the growth rate decreased to 4.2 nm h^{-1}. We hypothesize that this can be explained by the mechanism of the Z-group approach: As the RAFT CTA remains tethered to the surface while polymerization occurs in solution, the growing polymer chains undergo constant detachment and reattachment to the surface-tethered CTA (see Figure 1). The reattached polymer chains increase in molecular weight throughout the reaction. For each reattachment, there is increased steric hindrance to adjacent grafting sites on the surface, preventing attachment of other chains. As a result, the overall brush growth rate and thickness at 30 mol/L are lower than 15 mol/L.

To further support this hypothesis, we anticipated that the grafting density of the polymer brushes would decrease over time. To study this, swelling experiments were performed on the polystyrene (pS) brushes using thermal SI-RAFT (see experimental information).[70,71] The grafting density of the pS brushes was determined via *in situ* ellipsometry swelling experiments in toluene. Following previous theoretical studies,[65,66] the pS grafting density, σ can be calculated by

$$\sigma = \frac{\rho h_{dry} N_A}{m_0 N} \quad (1)$$

where ρ is the bulk density of the polymer, h_{dry} is the dry thickness of the polymer brush, N_A is Avogadro's number, and m_0 is the molecular weight of the monomer. The degree of polymerization, N, of pS brushes can be calculated by[66,67]

$$N = 1.074 \frac{(h_{swollen})^{3/2}}{(h_{dry}(Å)^2)^{1/2}} \quad (2)$$

where $h_{swollen}$ is the swollen thickness of the polymer brush, and h_{dry} is the dry thickness of the polymer brush. Table S1 provides the dry and equilibrium swollen thicknesses of pS brushes in ambient air and in toluene, respectively.

Figure 3 shows that indeed the grafting density of pS brushes decreased with reaction time. The initial grafting density

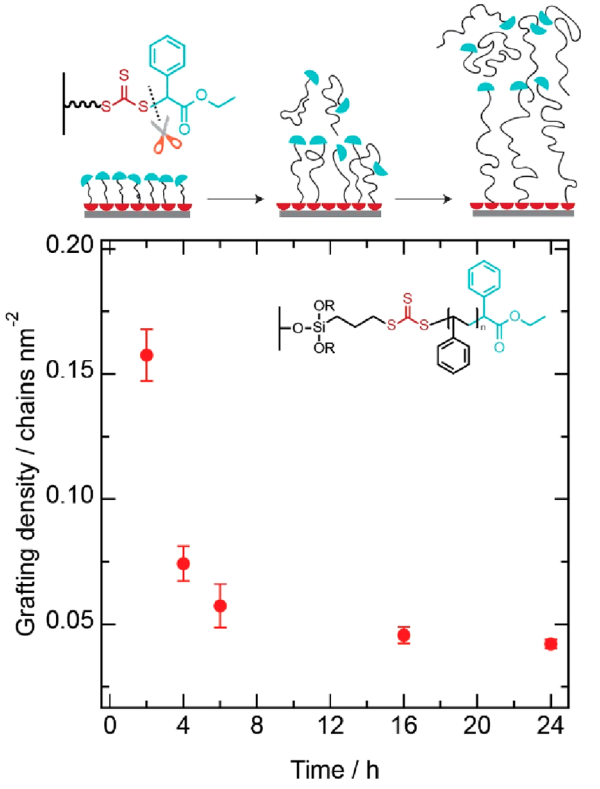

Figure 3. Grafting density of polystyrene brushes as a function of polymerization time for Z-group SI-RAFT (thermally initiated).

https://doi.org/10.1021/acspolymersau.3c00028
ACS Polym. Au 2023, 3, 428−436

obtained after 2 h of reaction time was determined to σ_{2h} = 0.16 ± 0.01 chains nm^{-2} i.e., less than our previous R-group approach; σ = 0.36 ± 0.05 chains nm^{-2}.[65] Over the course of the reaction, the grafting density decreased to σ_{24h} = 0.04 ± 0.001 chains nm^{-2}. This finding supports that increasing molecular weight in solution (detachment and reattachment equilibrium) leads to increased steric hindrance between the existing polymer chains at the surface and those trying to occupy adjacent sites. As a result, fewer polymer chains can be reattached to the substrates after degrafting and polymerization in solution.

2.3. Z-Group SI-PET-RAFT Monomer Scope

To study the scope of the outlined Z-group SI-PET-RAFT approach, we attempted polymerization with various inhibitor free monomers. Our study included: acrylamides (*N*-isopropylacrylamide (NIPAM)) and various methacrylates (using Ir(ppy)$_3$ as PC): methyl methacrylate (MMA), [poly(ethylene glycol) methyl ether methacrylate] (PEGMEMA), and 2,2,2-trifluoroethy methacrylate (TFEMA). The chemical composition of the individual homopolymer brushes was verified by XPS (see Figure S7). The presence of the N 1s peak at BE$_{N\ 1s}$ = 400 eV in the survey spectra confirmed the successful covalent attachment of p(NIPAM) on the substrates. For p(MMA), and p(PEGMEMA) the presence of carbonyl peak (O−C═O) at BE$_{O-C=O}$ = 289.0 eV, and the presence of C−O at BE$_{C-O}$ = 286.5 eV in the high-resolution carbon C 1s scan confirmed the covalent attachment of the polymer brushes to the substrate. For p(TFEMA) brushes, the presence of F 1s peak at BE$_{F\ 1s}$ = 688 eV in the survey spectrum and C−F$_3$ (BE$_{C-F3}$ = 292.9 eV) in the carbon C 1s spectrum also indicated successful formation of p(TFEMA) brushes. The XPS and theoretical atomic percentage ratios matched well within the experimental error for all monomers (see Table S2). The water contact angles (WCA) for the above homopolymers varied from θ = 42° to 105°, showing a broad range of surface wettability that can be obtained with this Z-group SI-PET-RAFT approach. For p(PEGMEMA) brushes, as a hydrophilic representative, the WCA was determined to $\theta_{pPEGMEMA}$= 42.4 ± 1.6°, whereas the WCA for p(TFEMA) was measured as θ_{pTFEMA} = 104.7 ± 1.9°. Figure S7 provides the WCAs for all homopolymers.

The SI-PET-RAFT via Z-group approach was further extended to ionic monomers using the aqueous SI-PET-RAFT polymerization under yellow light (λ = 590 nm).[61,70] For SI-PET-RAFT polymerizations in aqueous systems, a water-soluble analogue of ZnTPP was used: Zn(II) meso-tetra(4-sulfonatophenyl)porphyrin (ZnTPPS^{4-}). Ascorbic acid was used as an oxygen quencher, which readily reacts with reactive singlet oxygen generated during the photocatalytic process. Representative cationic, anionic, and zwitterionic monomers were chosen to study polymerization from the RAFT CTA-functionalized wafers: cationic [2-(methacrloyloxy)-ethyl] trimethylammonium chloride (METAC), anionic 3-sulfopropyl methacrylate potassium salt (SPMK), and zwitterionic 2-methacryloyloxyethyl phosphorylcholine (MPC). The chemical composition of the individual homopolymer brushes was verified by XPS (see Figure S8), and theoretical and experimental atomic % ratios matched well within experimental error (see Table S4). WCA measurements confirmed the expected hydrophilic nature of the resulting polyelectrolytic and polyzwitterionic coatings on the substrates (see Figure S8).

2.4. Chain Extension Using the Z-Group SI-PET-RAFT Approach

One of the important characteristics of RAFT is chain end retention. To examine chain end activity for this Z-group SI-PET-RAFT approach, chain extension experiments were performed on p(MMA) brushes using [M]:[PC] = 500:0.025 and [M]$_0$ = 15 mol/L (see Figure 4). After

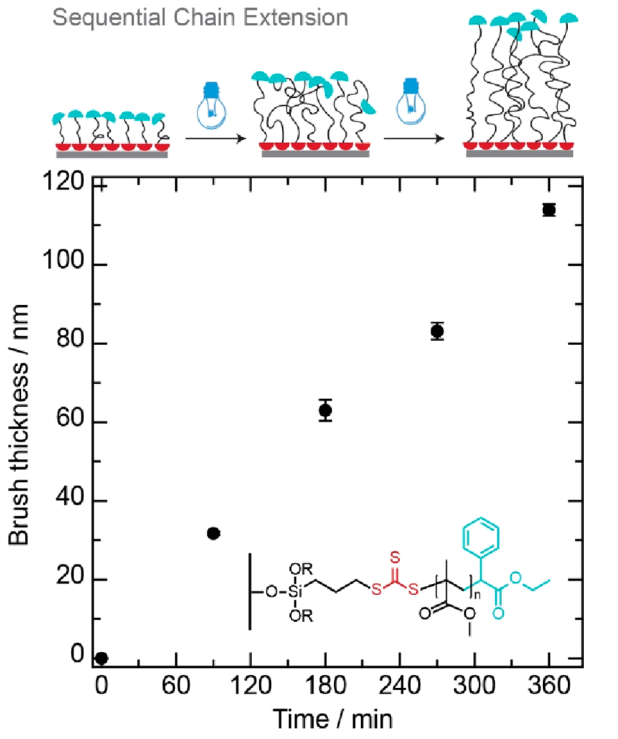

Figure 4. Polymer brush thickness vs irradiation time for chain extension of p(MMA) brushes with methyl methacrylate, using Ir(ppy)$_3$ as photocatalyst under λ = 405 nm wavelength light.

polymerizing an initial p(MMA) layer for 90 min, the reaction was stopped by turning off the light source. Following this, the substrate was rinsed with dichloromethane to remove any remaining unreacted monomer and physisorbed polymer chains. Subsequently, a freshly prepared solution containing the monomer and PC was added to the same wafer. By repeating this procedure, it was possible to obtain p(MMA) polymer brush layers with thickness of up to d = 113.9 ± 1.5 nm. The sequential extension follows a linear relationship of thickness versus time (see Figure 4). Grafting density experiments on p(MMA) chain-extended brushes again showed a decrease in the grafting density with increasing reaction time (and thickness). As shown in Figure S6, the initial grafting density obtained after 1.5 h of reaction time was determined as $\sigma_{1.5h}$ = 0.0425 ± 0.002 chains nm^{-2}. Over the course of the chain extensions, grafting density decreased to $\sigma_{4.5h}$ = 0.0129 ± 0.0005 chains nm^{-2}. This further corroborates our hypothesized SI-PET-RAFT mechanism of increasing p(MMA) molecular weight in solution and the detachment/reattachment equilibrium resulting in increased steric hindrance between the adjacent grafting sites at the surface.

2.5. Diblock Copolymer Extension Using SI-PET-RAFT via the Z-Group Approach

A unique feature of the Z-group SI-RAFT mechanism is the ability to modify the layers between a polymer brush and

https://doi.org/10.1021/acspolymersau.3c00028
ACS Polym. Au 2023, 3, 428−436

substrate. We anticipated that if we perform a diblock copolymerization, the second block will grow *underneath* the first layer (see Figures 1 and 5). Diblock copolymerization

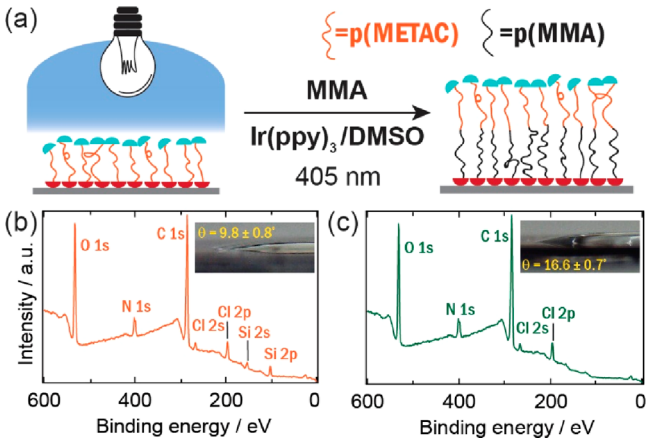

Figure 5. (a) Schematic of the synthesis of l-p(MMA)-*b*-p(METAC) diblock copolymer brushes. XPS survey spectra (b) before (inset WCA image) and (c) after (inset WCA image) the diblock copolymer brushes.

experiments were performed with METAC and MMA monomers. Beginning with an initial p(METAC) brush film ($d_{p(METAC)}$ = 7 nm) we added a solution of MMA, and PC to synthesize p(METAC-*b*-MMA) diblock copolymer brushes (see Figure 5a).

Indeed, XPS and WCA measurements provided evidence that the outermost surface of the new diblock polymer brush was not changed significantly. The thickness of l-p(MMA)-*b*-p(METAC) changed from an initial value of $d_{p(METAC)}$ = 7 nm to $d_{p(MMA)\text{-}b\text{-}(METAC)}$ = 17 nm. However, the WCA measurements (see Figure 5b, c) before (θ = 9.8 ± 0.8°) and after (θ = 16.6 ± 0.7°) diblock copolymerization did not change significantly, suggesting that the top layer remains the p(METAC) block. Further evidence that the p(MMA) block was grown between the p(METAC) layer and the substrate was gathered through XPS:METAC-characteristic N 1s, Cl 2s, and Cl 2p peaks at $BE_{N\ 1s}$ = 400 eV, $BE_{Cl\ 2s}$ = 269 eV, and $BE_{Cl\ 2p}$ = 200 eV, respectively, which were identified both before *and* after the diblock copolymer brush polymerization (see Figure 5b). Simultaneously, and in agreement with the increased film thickness, the substrate-specific Si 2s, and Si 2p peaks at $BE_{Si\ 2s}$ = 150 eV, and $BE_{Si\ 2p}$ = 102 eV (see Figure 5c) disappeared. Beyond these peaks, the XPS elemental compositions before and after the diblock growth were also similar to the theoretical values (see Table S5). Therefore, these results provide further experimental evidence of the Z-group mechanism and the incorporation of a p(MMA) block *between* the p(METAC) block and the surface. Notably, this contrasts with the previously established R-group SI-PET-RAFT approach,[60] now allowing growth of intermittent polymer brush layers underneath a top layer without changing the properties of the outermost surface.

2.6. Photolithography and Cross-Patterning

As a light-mediated technique, SI-PET-RAFT provides the ability to obtain spatial control over the polymer brush growth. Polymer brush patterning studies on silicon wafers were performed by using DMA as the monomer and ZnTPP as the photocatalyst ([M]:[PC] = 500:0.025, and [M] = 15 mol/L in DMSO). A striped photomask was used (5 μm line spacing) under visible light irradiation (λ = 405 nm). As was described previously, the achievable spatial resolution for this visible light-mediated approach is diffraction-limited, theoretically allowing for a spatial pattern resolution of approximately $\lambda/2$ of the light used.[68,69] Figure 6b shows the optical micrographs of

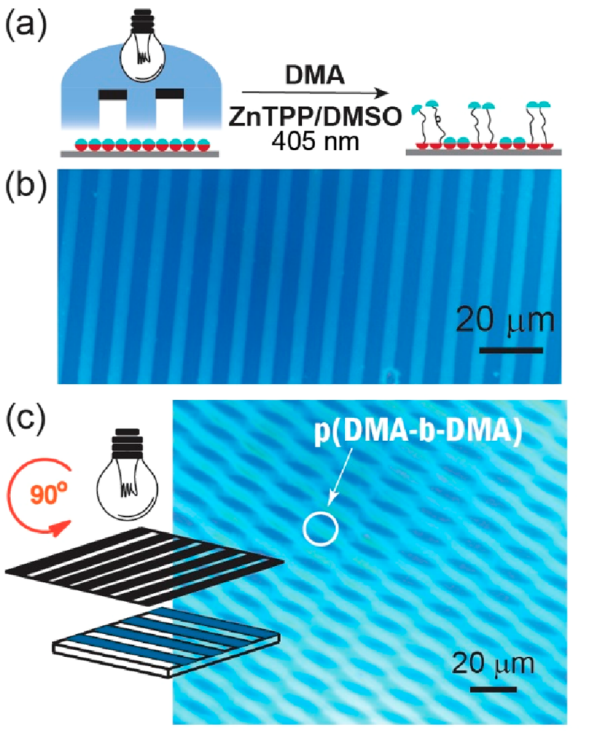

Figure 6. (a) Schematics of the polymer brush photolithography. Optical micrographs of (b) initial striped-patterned p(DMA) layer and (c) cross-patterned p(DMA) extension p(DMA-*b*-DMA) using a photomask with 5 μm line spacing.

the resulting patterned p(DMA) brush surface. We also investigated chain end retention by the sequential cross-patterning of a second p(DMA) brush layer. The optical micrograph in Figure 6c confirmed successful cross-patterning of l-p(DMA-*b*-DMA), providing evidence that this approach enables complex patterning on substrates. Patterning experiments were also performed with different monomers, and all resulting optical micrographs showed successful patterning (see Figure S9).

3. CONCLUSION

In conclusion, we described a light-mediated Z-group approach towards SI-PET-RAFT photopolymerization. The outlined technique provided controlled growth and chain extension capabilities and allowed for chemical patterning of surfaces by using visible light under ambient conditions. Thermally initiated SI-RAFT was also performed from the Z-group-tethered RAFT CTA, which provided the compatibility of this approach to leverage both thermally and light-mediated surface-initiated polymerizations. The versatility of this technique was explored while changing the photocatalyst, wavelength of light, and monomers, which included various acrylamides and methacrylates. This technique was also extended to aqueous, oxygen-tolerant SI-PET-RAFT and three different ionic monomers were successfully polymerized

https://doi.org/10.1021/acspolymersau.3c00028
ACS Polym. Au 2023, 3, 428−436

in water and under visible light irradiation under ambient conditions. The developed approach also allowed for sequential chain-extensions with the same monomer and diblock copolymerization with two different monomers. The polymer brush growth rate with this approach was $dd/dt = 5.4$ nm h^{-1}, which was less than our previous SI-PET-RAFT via R-group approach $dd/dt = 25$ nm h^{-1}. Finally, the grafting density was shown to decrease with time, confirming the proposed Z-group mechanism of a detachment/reattachment equilibrium of polymer brushes. While the grafting density with R-group SI-PET-RAFT approach was measured to be around 0.36 ± 0.05 chains nm^{-2}, the Z-group approach described the herein yields lower grafting densities that vary with reaction time (from 0.013 to 0.160 chains nm^{-2}).

4. EXPERIMENTAL SECTION

4.1. Materials

The following chemicals were purchased from Sigma-Aldrich and used as received: Styrene, *N*,*N*-dimethyl acrylamide (DMA), *N*-isopropylacrylamide (NIPAM), methyl methacrylate (MMA), poly(ethylene glycol) methyl ether methacrylate (PEGMEMA), 2,2,2-trifluoroethyl methacrylate (TFEMA), [2-(methacryloyloxy)ethyl]-trimethylammonium chloride solution (75 wt % in H_2O; METAC), 3-sulfopropyl methacrylate potassium salt (SPMK), 2-methacryloyloxyethyl phosphorylcholine (MPC), anhydrous methanol, sodium methoxide (25 wt % in methanol), carbon disulfide, ethyl α-bromophenylacetate (EBrPA), 5,10,15,20-tetraphenyl- 21*H*,23*H*-porphine zinc (ZnTPP), tris(2-phenylpyridine)iridium(III) (fac-Ir(ppy)$_3$]), 2,2′-azobis(2-methylpropionitrile) (AIBN), and dimethyl sulfoxide (DMSO). Methylene chloride (DCM), toluene, tetrahydrofuran (THF), isopropyl alcohol, acetone, methanol, 3-(mercaptopropyl) triethoxysilane (MPTES), and ascorbic acid were purchased from Fisher Scientific. Zn(II) meso-tetra(4-sulfonatophenyl) porphyrin ($ZnTPPS^{4-}$) was obtained from Fronteir Scientific and used as received. House deionized (DI) water was used from Penn State University's Chemical and Biomedical Engineering building. Silicon wafers (with native oxide and 100 nm thermal oxide layers) were purchased from WaferPro, LLC (San Jose, CA). A striped photomask was purchased from Photronics, Inc. (Brookfield, CT). A patterning photomask was designed by in-house NanoFab laboratory from the Penn State University's Materials Research Institute. LED light strips (λ = 405 and λ = 590 nm) were purchased from LEDlightinghut.com. Thorlabs Olympus BX & IX series (λ = 365 nm) collimated LEDs were modulated by a Thorlabs LED D1B T-cube driver and used to degrarde RAFT CTAs on functionalized wafers. Light intensities were determined using a TRENDBOX digital light meter purchased from Amazon.

4.2. Characterization

^{1}H Nuclear Magnetic Resonance (NMR) spectroscopy measurements were performed on a Bruker AVIII-HD-500 MHz instrument. The chemical shifts are reported in δ (ppm) and are referenced to the characteristic peak for deuterated $CDCl_3$ at δ = 7.26 ppm.

X-ray photoelectron spectroscopy (XPS) spectra were acquired by using a Physical Electronics VersaProbe III spectrometer, utilizing a monochromatic Al Kα X-ray source at an energy of 1486.6 eV under a vacuum of 10^{-8} Torr. CasaXPS (Casa Software Ltd.) was used to analyze the photoelectron spectra. For visualization of patterned surfaces, a Carl Zeiss Axio Scope A1 microscope was used with an Axiocam 305 color camera.

Variable-angle spectroscopic ellipsometry (VASE) was performed using a J.A. Woollam RC2 instrument at incident angles of 55°, 65°, and 75° (wavelength range: 193−1000 nm) was used to characterize the thickness of polymer brushes on silicon substrates. From the measured data, film thicknesses and optical constants were fitted using CompleteEASE software (J.A. Woollam Co., Inc.) and a three-layer model: (1) a silicon base substrate layer, (2) a native SiO_2 layer with a thickness of 1.55 nm (native oxide) or 100 nm (thermal oxide), and (3) a polymer layer. Either B-Spline or Gen-Osc models containing several Gaussian generalized oscillators were used to fit the VASE data. Ellipsometry was used to evaluate the swelling behavior of polymer brushes using a 500 μL horizontal liquid cell with a window angle of 70°. After the solvent was injected, data collection began and the sample was equilibrated; i.e., the thickness did not fluctuate significantly for 30 min. The final thickness was recorded as the swollen thickness ($h_{swollen}$). Cauchy models were used to fit the optical properties and thickness of the polymer brush layers using data collected at wavelengths between 400 and 1000 nm. The optical constants of the solvents (THF and toluene) were determined on a calibration wafer with a known SiO_2 layer thickness and optical constant. The following Cauchy parameters were used for toluene: A = 1.474, B = 0.00440, C = 0.0047487 and for THF: A = 1.392, B = 0.00256, C = 0.00011921. The D_2 lamp (UV light source) was switched off to protect the polymer brush film from degradation during the in situ measurements, and only the visible light QTH lamp was used.

Tensiometry was performed by using a custom-built setup involving a webcam (Hotpet 5 MPixel webcam) and a planoconvex lens with a focal length of 50 mm. A sample was placed on top of a platform and 5 μL of DI water was carefully deposited using a micropipette. A fluorescent utility lamp was used to provide backlight and a webcam was used to capture clear focused photographs of the sessile drop. Prior to measurements, the samples were thoroughly dried using a compressed air stream. Values were averaged between three different measurements at three different locations on the surface. From the images, the water contact angle (WCA) was determined using the "*Both Bestfits*" option within an ImageJ plugin developed by Marco Brugnara (available at https://imagej.nih.gov/ij/index.html).

4.3. Synthesis of RAFT CTA

The synthesis of the RAFT CTA was performed based on a previously published procedure.[56] 3-(Mercaptopropyl) triethoxysilane (1.90 g, 7.5 mol) and 13 mL of anhydrous methanol were added to a 100 mL round-bottom flask equipped with a magnetic stir bar and rubber septum. The mixture was degassed through sparging and moved into a glovebox (nitrogen atmosphere). Sodium methoxide (25 wt % in methanol, 1.62 g, 30 mmol) was added dropwise under nitrogen atmosphere. After the mixture was stirred for 30 min, carbon disulfide (0.76 g, 10 mmol) was added dropwise, and the mixture was stirred at ambient temperature and under nitrogen for 5 h. To this yellow solution was added ethyl α-bromophenylacetate (1.86 g, 7.5 mmol) dropwise, and the mixture was stirred for 16 h under nitrogen. The crude mixture was concentrated in vacuo, diluted with dichloromethane, filtered, and concentrated in vacuo to provide a viscous orange-yellow liquid (Yield: 74%). ^{1}H NMR (500 MHz, $CDCl_3$, 25 °C, δ, ppm): 0.74 (t, 2H), 1.24 (t, 12H), 1.81 (m, 2H), 3.37 (t, 2H), 3.6 (q, 6H), 4.22 (m, 2H), 5.80 (s, 1H), 7.34 (m, 5H).

4.4. Preparation of RAFT CTA-Functionalized Surfaces

Preparation of RAFT CTA-functionalized surfaces was adapted from our previous procedures.[70] Silicon substrates (either with a native oxide layer of 1.55 nm or 100 nm thermal oxide) were cut into square pieces off approximately 1.5 cm × 1.5 cm. The substrates were cleaned by ultrasonication in toluene and isopropanol (10 min each) dried under a stream of N_2. The SiO_2 wafers were then activated for 15 min in air plasma (300 mTorr) using a PDC-001 plasma cleaner (Harrick Plasma) before they were immersed for 40 h in a freshly prepared solution containing 30 μL of the synthesized RAFT CTA in 50 mL of dry toluene at room temperature. The RAFT CTA functionalized wafers were rinsed with toluene and isopropanol, dried under nitrogen gas, and stored in a glovebox for further use.

4.5. General Procedures for SI-PET-RAFT in DMSO, Patterning, and Chain Extension Experiments

Generalized procedures for SI-PET-RAFT were followed as outlined previously by our group.[70] All surface-initiated polymerizations were performed by positioning the RAFT CTA functionalized substrates approximately 6 cm below the LED light source. Experiments were

https://doi.org/10.1021/acspolymersau.3c00028
ACS Polym. Au 2023, 3, 428−436

performed either in a glovebox (MBRAUN, LABstar pro) or in a fume hood (open to air). A stock solution of 1 mg of photocatalysts ($Ir(ppy)_3$ or ZnTPP) dissolved in 1 mL of DMSO was prepared and kept in the dark to avoid photobleaching. Monomers were purified by using a basic alumina column to remove the inhibitor. An SI-PET-RAFT polymerization solution was prepared by mixing the monomer (inhibitor removed) and the photocatalyst stock solution at a molar ratio of [M]:[PC] = 500:0.025. The solution was pipetted onto a RAFT CTA functionalized SiO_2 wafer and covered using a glass coverslip to create a thin reaction mixture layer. Samples were irradiated at λ = 405 nm for the desired reaction time using an LED light source to activate the photocatalysts (intensity: 2400 lx). For photolithography experiments, a patterned photomask was placed on top of the wafer instead of a covers slip. Following the reaction, the substrates were cleaned with dichloromethane (DCM) to remove the physisorbed polymer and excess reaction solution, isopropyl alcohol, and dried under N_2 gas. Finally, for chain extension experiments, a freshly prepared reaction solution of MMA and photocatalyst/DMSO solution (see above) was used for each reaction.

4.5.1. SI-PET-RAFT in DMSO: Control Experiments and Degrading Initiators Prior to Growing Polymer Brushes. A patterned photomask was placed on top of a RAFT CTA-functionalized wafer and a UV light (Thorlabs Olympus BX & IX series, λ = 365 nm) was used to irradiate the substrate for 16 h. Subsequently, the wafers were cleaned with isopropyl alcohol and dried under a stream of nitrogen. Subsequently, an SI-PET-RAFT procedure was performed as outlined in above. Optical microscopy was used to visualize the resulting topographical patterning.

4.5.2. SI-RAFT of Styrene on MPTES-EBrPA Functionalized Wafers. After the inhibitor was removed by passing styrene through a basic alumina column, a RAFT reaction mixture was prepared by mixing styrene (M) and 2,2′-azobis(2-methylpropionitrile) (AIBN) at a molar ratio of [M]:[AIBN] = 400:0.2. In a 20 mL vial, the RAFT CTA functionalized wafer was submerged in the resulting reaction mixture and sparged with nitrogen for 10 min. The vials were heated at 75 °C for the targeted reaction time before the reaction terminated by placing the vial in an ice bath for 10 min. Finally, the wafers were cleaned thoroughly with toluene and dried with nitrogen gas.

4.5.3. General Procedure for SI-PET-RAFT in Water. Polymerization procedures were adapted following a previous procedure from our group.[70] Initially, a stock solution was prepared, consisting of 1 mg of photocatalyst $ZnTPPS^{4-}$ dissolved in 1 mL of DI water and then kept in a dark environment. A reaction mixture was prepared by mixing the inhibitor-free monomer, ascorbic acid, and the photocatalyst/DI water stock solution at a molar ratio of [monomer]:[ascorbic acid]:[photocatalyst] = 500:2:0.025 for all liquid monomers. Solid monomers (SPMK and MPC) were polymerized using a reaction mixture solution with at a molar ratio of [monomer]:[ascorbic acid]:[photocatalyst] = 500:2:0.05. Additional $ZnTPPS^{4-}$/DI water stock solution was used to dissolve the monomers in this case. This reaction mixture was then pipetted onto a RAFT CTA functionalized wafer. Then, a glass coverslip was placed on top of the wafer to create a thin layer of reaction mixture. The samples were irradiated with a light source of λ = 590 nm, having an intensity of 4600 lx for a specified duration. Following irradiation, the wafers were cleaned thoroughly with DI water and isopropyl alcohol and dried using nitrogen gas.

■ ASSOCIATED CONTENT

Supporting Information

The Supporting Information is available free of charge at https://pubs.acs.org/doi/10.1021/acspolymersau.3c00028.

Materials and instrumentation details, NMR and XPS characterization details of the RAFT CTA product and functionalized substrates, respectively; influence of monomer to solvent concentration on the kinetics of polymer brush growth; details on control experiments; grafting density studies of chain extended brushes; XPS and water contact angle characterization data of various polymer brush films; photopatterning micrographs; and examples for ellipsometry modeling (PDF)

■ AUTHOR INFORMATION

Corresponding Author

Christian W. Pester − *Department of Chemical Engineering and Department of Materials Science and Engineering, Department of Chemistry, The Pennsylvania State University, University Park, Pennsylvania 16802, United States;* orcid.org/0000-0001-7624-4165; Email: pester@psu.edu

Author

Sai Dileep Kumar Seera − *Department of Chemical Engineering, The Pennsylvania State University, University Park, Pennsylvania 16802, United States*

Complete contact information is available at: https://pubs.acs.org/10.1021/acspolymersau.3c00028

Author Contributions

CRediT: **Sai Dileep Kumar Seera** data curation, formal analysis, investigation, validation, visualization, writing-original draft, writing-review & editing.

Notes

The authors declare no competing financial interest.

■ ACKNOWLEDGMENTS

We would like to acknowledge Corning Inc. for financial support and Jeff Shallenberger and the Penn State Material Characterization laboratory for assistance with XPS experiments.

■ REFERENCES

(1) Thompson, L.F.; Willson, C. G.; Bowden, M.J.. *Introduction to Microlithography*; American Chemical Society, Washington DC, 1994.

(2) Teramura, Y.; Iwata, H. Cell Surface Modification with Polymers for Biomedical Studies. *Soft Matter* **2010**, *6* (6), 1081−1091.

(3) Kango, S.; Kalia, S.; Celli, A.; Njuguna, J.; Habibi, Y.; Kumar, R. Surface Modification of Inorganic Nanoparticles for Development of Organic-Inorganic Nanocomposites - A Review. *Prog. Polym. Sci.* **2013**, *38* (8), 1232−1261.

(4) Dash, J. G.. *Films on Solid Surfaces: The Physics and Chemistry of Physical Adsorption*; Academic Press, 1975.

(5) Milner, S. T. Polymer Brushes. *Science* **1991**, *251* (4996), 905−914.

(6) Brittain, W. J.; Minko, S. A Structural Definition of Polymer Brushes. *J. Polym. Sci., Part A: Polym. Chem.* **2007**, *45* (16), 3505−3512.

(7) Barbey, R.; Lavanant, L.; Paripovic, D.; Schüwer, N.; Sugnaux, C.; Tugulu, S.; Klok, H. A. Polymer Brushes via Surface-Initiated Controlled Radical Polymerization: Synthesis, Characterization, Properties, and Applications. *Chem. Rev.* **2009**, *109* (11), 5437−5527.

(8) Welch, M. E.; Ober, C. K. Responsive and Patterned Polymer Brushes. *J. Polym. Sci., Part B: Polym. Phys.* **2013**, *51* (20), 1457−1472.

(9) Chen, T.; Ferris, R.; Zhang, J.; Ducker, R.; Zauscher, S. Stimulus-Responsive Polymer Brushes on Surfaces: Transduction Mechanisms and Applications. *Progress in Polymer Science (Oxford)* **2010**, *35* (1−2), 94−112.

(10) Minko, S. Responsive Polymer Brushes. *Polym. Rev.* **2006**, *46* (4), 397−420.

(11) Krishnamoorthy, M.; Hakobyan, S.; Ramstedt, M.; Gautrot, J. E. Surface-Initiated Polymer Brushes in the Biomedical Field:

Applications in Membrane Science, Biosensing, Cell Culture, Regenerative Medicine and Antibacterial Coatings. *Chem. Rev.* **2014**, *114* (21), 10976−11026.
(12) Pester, C. W.; Poelma, J. E.; Narupai, B.; Patel, S. N.; Su, G. M.; Mates, T. E.; Luo, Y.; Ober, C. K.; Hawker, C. J.; Kramer, E. J. Ambiguous Anti-Fouling Surfaces: Facile Synthesis by Light-Mediated Radical Polymerization. *J. Polym. Sci., Part A: Polym. Chem.* **2016**, *54*, 253−262.
(13) Ng, G.; Li, M.; Yeow, J.; Jung, K.; Pester, C. W.; Boyer, C. Benchtop Preparation of Polymer Brushes by SI-PET-RAFT: The Effect of the Polymer Composition and Structure on Inhibition of a Pseudomonas Biofilm. *ACS Appl. Mater. Interfaces* **2020**, *12* (49), 55243−55254.
(14) Ng, G.; Judzewitsch, P.; Li, M.; Pester, C. W.; Jung, K.; Boyer, C. Synthesis of Polymer Brushes Via SI-PET-RAFT for Photodynamic Inactivation of Bacteria. *Macromol. Rapid Commun.* **2021**, *42* (18), 1−6.
(15) Poisson, J.; Polgar, A. M.; Fromel, M.; Pester, C. W.; Hudson, Z. M. Preparation of Patterned and Multilayer Thin Films for Organic Electronics via Oxygen-Tolerant SI-PET-RAFT. *Angewandte Chemie - International Edition* **2021**, *60* (36), 19988−19996.
(16) Page, Z. A.; Narupai, B.; Pester, C. W.; Bou Zerdan, R.; Sokolov, A.; Laitar, D. S.; Mukhopadhyay, S.; Sprague, S.; McGrath, A. J.; Kramer, J. W.; Trefonas, P.; Hawker, C. J. Novel Strategy for Photopatterning Emissive Polymer Brushes for Organic Light Emitting Diode Applications. *ACS Cent Sci.* **2017**, *3* (6), 654−661.
(17) Narupai, B.; Page, Z. A.; Treat, N. J.; McGrath, A. J.; Pester, C. W.; Discekici, E. H.; Dolinski, N. D.; Meyers, G. F.; Read de Alaniz, J.; Hawker, C. J. Simultaneous Preparation of Multiple Polymer Brushes under Ambient Conditions Using Microliter Volumes. *Angewandte Chemie - International Edition* **2018**, *57* (41), 13433−13438.
(18) Hu, H.; Yu, B.; Ye, Q.; Gu, Y.; Zhou, F. Modification of Carbon Nanotubes with a Nanothin Polydopamine Layer and Polydimethylamino-Ethyl Methacrylate Brushes. *Carbon* **2010**, *48* (8), 2347−2353.
(19) Long, W.; Jones, C. W. Hybrid Sulfonic Acid Catalysts Based on Silica-Supported Poly(Styrene Sulfonic Acid) Brush Materials and Their Application in Ester Hydrolysis. *ACS Catal.* **2011**, *1* (7), 674−681.
(20) Bell, K.; Freeburne, S.; Fromel, M.; Oh, H. J.; Pester, C. W. Heterogeneous Photoredox Catalysis Using Fluorescein Polymer Brush Functionalized Glass Beads. *J. Polym. Sci.* **2021**, *59* (22), 2844−2853.
(21) Bell, K.; Freeburne, S.; Wolford, A.; Pester, C. W. Reusable Polymer Brush-Based Photocatalysts for PET-RAFT Polymerization. *Polym. Chem.* **2022**, *13* (43), 6120−6126.
(22) Bell, K.; Guo, Y.; Barker, S.; Kim, S. H.; Pester, C. W. Thermoresponsive Polymer Brush Photocatalytic Substrates for Wastewater Remediation. *Polym. Chem.* **2023**, *14* (22), 2662−2669.
(23) Bell, K.; Hunter, B.; Alvarez, M.; Seera, S. D. K.; Guo, Y.; Lin, Y. T.; Kim, S. H.; Pester, C. W. Hydrolysis-Resistant Heterogeneous Photocatalysts for PET-RAFT Polymerization in Aqueous Environments. *J. Mater. Chem. A Mater.* **2023**, *11* (31), 16616−16625.
(24) Welch, M.; Rastogi, A.; Ober, C. Polymer Brushes for Electrochemical Biosensors. *Soft Matter* **2011**, *7* (2), 297−302.
(25) Degirmenci, A.; Yeter Bas, G.; Sanyal, R.; Sanyal, A. clickable" Polymer Brush Interfaces: Tailoring Monovalent to Multivalent Ligand Display for Protein Immobilization and Sensing. *Bioconjugate Chem.* **2022**, *33* (9), 1672−1684.
(26) Badoux, M.; Billing, M.; Klok, H. A. Polymer Brush Interfaces for Protein Biosensing Prepared by Surface-Initiated Controlled Radical Polymerization. *Polym. Chem.* **2019**, *10* (23), 2925−2951.
(27) Hess, L. H.; Lyuleeva, A.; Blaschke, B. M.; Sachsenhauser, M.; Seifert, M.; Garrido, J. A.; Deubel, F. Graphene Transistors with Multifunctional Polymer Brushes for Biosensing Applications. *ACS Appl. Mater. Interfaces* **2014**, *6* (12), 9705−9710.
(28) Zoppe, J. O.; Ataman, N. C.; Mocny, P.; Wang, J.; Moraes, J.; Klok, H. A. Surface-Initiated Controlled Radical Polymerization: State-of-the-Art, Opportunities, and Challenges in Surface and Interface Engineering with Polymer Brushes. *Chem. Rev.* **2017**, *117* (3), 1105−1318.
(29) Chen, W. L.; Cordero, R.; Tran, H.; Ober, C. K. 50th Anniversary Perspective: Polymer Brushes: Novel Surfaces for Future Materials. *Macromolecules* **2017**, *50* (11), 4089−4113.
(30) Poelma, J. E.; Fors, B. P.; Meyers, G. F.; Kramer, J. W.; Hawker, C. J. Fabrication of Complex Three-Dimensional Polymer Brush Nanostructures through Light-Mediated Living Radical Polymerization. *Angewandte Chemie - International Edition* **2013**, *52* (27), 6844−6848.
(31) Pan, X.; Fantin, M.; Yuan, F.; Matyjaszewski, K. Externally Controlled Atom Transfer Radical Polymerization. *Chem. Soc. Rev.* **2018**, *47* (14), 5457−5490.
(32) Fromel, M.; Li, M.; Pester, C. W. Surface Engineering with Polymer Brush Photolithography. *Macromol. Rapid Commun.* **2020**, *41* (18), 1−17.
(33) Matyjaszewski, K.; Dong, H.; Jakubowski, W.; Pietrasik, J.; Kusumo, A. Grafting from Surfaces for "Everyone": ARGET ATRP in the Presence of Air. *Langmuir* **2007**, *23* (8), 4528−4531.
(34) Min, K.; Jakubowski, W.; Matyjaszewski, K. AGET ATRP in the Presence of Air in Miniemulsion and in Bulk. *Macromol. Rapid Commun.* **2006**, *27* (8), 594−598.
(35) Discekici, E. H.; Pester, C. W.; Treat, N. J.; Lawrence, J.; Mattson, K. M.; Narupai, B.; Toumayan, E. P.; Luo, Y.; McGrath, A. J.; Clark, P. G.; Read De Alaniz, J.; Hawker, C. J. Simple Benchtop Approach to Polymer Brush Nanostructures Using Visible-Light-Mediated Metal-Free Atom Transfer Radical Polymerization. *ACS Macro Lett.* **2016**, *5* (2), 258−262.
(36) Narupai, B.; Page, Z. A.; Treat, N. J.; McGrath, A. J.; Pester, C. W.; Discekici, E. H.; Dolinski, N. D.; Meyers, G. F.; Read de Alaniz, J.; Hawker, C. J. Simultaneous Preparation of Multiple Polymer Brushes under Ambient Conditions Using Microliter Volumes. *Angewandte Chemie - International Edition* **2018**, *57* (41), 13433−13438.
(37) Fromel, M.; Benetti, E. M.; Pester, C. W. Oxygen Tolerance in Surface-Initiated Reversible Deactivation Radical Polymerizations: Are Polymer Brushes Turning into Technology? *ACS Macro Lett.* **2022**, *11* (4), 415−421.
(38) Narupai, B.; Poelma, J. E.; Pester, C. W.; McGrath, A. J.; Toumayan, E. P.; Luo, Y.; Kramer, J. W.; Clark, P. G.; Ray, P. C.; Hawker, C. J. Hierarchical Comb Brush Architectures via Sequential Light-Mediated Controlled Radical Polymerizations. *J. Polym. Sci., Part A: Polym. Chem.* **2016**, *54* (15), 2276−2284.
(39) Pester, C. W.; Narupai, B.; Mattson, K. M.; Bothman, D. P.; Klinger, D.; Lee, K. W.; Discekici, E. H.; Hawker, C. J. Engineering Surfaces through Sequential Stop-Flow Photopatterning. *Adv. Mater.* **2016**, *28* (42), 9292−9300.
(40) Matyjaszewski, K.; Miller, P. J.; Shukla, N.; Immaraporn, B.; Gelman, A.; Luokala, B. B.; Siclovan, T. M.; Kickelbick, G.; Valiant, T.; Hoffmann, H.; Pakula, T. Polymers at Interfaces: Using Atom Transfer Radical Polymerization in the Controlled Growth of Homopolymers and Block Copolymers from Silicon Surfaces in the Absence of Untethered Sacrificial Initiator. *Macromolecules* **1999**, *32* (26), 8716−8724.
(41) Pyun, J.; Kowalewski, T.; Matyjaszewski, K. Synthesis of Polymer Brushes Using Atom Transfer Radical Polymerization. *Macromol. Rapid Commun.* **2003**, *24* (18), 1043−1059.
(42) Baum, M.; Brittain, W. J. Synthesis of Polymer Brushes on Silicate Substrates via Reversible Addition Fragmentation Chain Transfer Technique. *Macromolecules* **2002**, *35* (3), 610−615.
(43) Husseman, M.; Malmström, E. E.; McNamara, M.; Mate, M.; Mecerreyes, D.; Benoit, D. G.; Hedrick, J. L.; Mansky, P.; Huang, E.; Russell, T. P.; Hawker, C. J. Controlled Synthesis of Polymer Brushes by "Living" Free Radical Polymerization Techniques. *Macromolecules* **1999**, *32* (5), 1424−1431.
(44) De Boer, B.; Simon, H. K.; Werts, M. P. L.; Van Der Vegte, E. W.; Hadziioannou, G. 'Living' Free Radical Photopolymerization

https://doi.org/10.1021/acspolymersau.3c00028
ACS Polym. Au 2023, 3, 428−436

Initiated from Surface-Grafted Iniferter Monolayers. *Macromolecules* **2000**, *33* (2), 349−356.
(45) Valles, D. J.; Zholdassov, Y. S.; Braunschweig, A. B. Evolution and Applications of Polymer Brush Hypersurface Photolithography. *Polym. Chem.* **2021**, *12* (40), 5724−5746.
(46) Kitano, H.; Liu, Y.; Tokuwa, K. I.; Li, L.; Iwanaga, S.; Nakamura, M.; Kanayama, N.; Ohno, K.; Saruwatari, Y. Polymer Brush with Pendent Glucosylurea Groups Constructed on a Glass Substrate by RAFT Polymerization. *Eur. Polym. J.* **2012**, *48* (11), 1875−1882.
(47) Bain, E. D.; Dawes, K.; Özçam, A. E.; Hu, X.; Gorman, C. B.; Šogl, J.; Genzer, J. Surface-Initiated Polymerization by Means of Novel, Stable, Non-Ester-Based Radical Initiator. *Macromolecules* **2012**, *45* (9), 3802−3815.
(48) Li, C.; Han, J.; Ryu, C. Y.; Benicewicz, B. C. A Versatile Method to Prepare RAFT Agent Anchored Substrates and the Preparation of PMMA Grafted-Nanoparticles. *Macromolecules* **2006**, *39* (9), 3175−3183.
(49) Günay, K. A.; Schüwer, N.; Klok, H. A. Synthesis and Post-Polymerization Modification of Poly(Pentafluorophenyl Methacrylate) Brushes. *Polym. Chem.* **2012**, *3* (8), 2186−2192.
(50) Matsuzaka, N.; Nakayama, M.; Takahashi, H.; Yamato, M.; Kikuchi, A.; Okano, T. Terminal-Functionality Effect of Poly(N -Isopropylacrylamide) Brush Surfaces on Temperature-Controlled Cell Adhesion/Detachment. *Biomacromolecules* **2013**, *14* (9), 3164−3171.
(51) Perrier, S.; Takolpuckdee, P.; Mars, C. A. Reversible Addition−Fragmentation Chain Transfer Polymerization Mediated by a Solid Supported Chain Transfer Agent. *Macromolecules* **2005**, *38* (16), 6770−6774.
(52) Takolpuckdee, P.; Mars, C. A.; Perrier, S. Merrifield Resin-Supported Chain Transfer Agents, Precursors for RAFT Polymerization. *Org. Lett.* **2005**, *7* (16), 3449−3452.
(53) Nguyen, D. H.; Vana, P. Silica-Immobilized Cumyl Dithiobenzoate as Mediating Agent in Reversible Addition Fragmentation Chain Transfer (RAFT) Polymerization. *Polym. Adv. Technol.* **2006**, *17* (9−10), 625−633.
(54) Stenzel, M. H.; Zhang, L.; Huck, W. T. S. Temperature-Responsive Glycopolymer Brushes Synthesized via RAFT Polymerization Using the Z-Group Approach. *Macromol. Rapid Commun.* **2006**, *27* (14), 1121−1126.
(55) Zhao, Y.; Perrier, S. Synthesis of Well-Defined Homopolymer and Diblock Copolymer Grafted onto Silica Particles by Z-Supported RAFT Polymerization. *Macromolecules* **2006**, *39* (25), 8603−8608.
(56) Zhao, Y.; Perrier, S. Reversible Addition-Fragmentation Chain Transfer Graft Polymerization Mediated by Fumed Silica Supported Chain Transfer Agents. *Macromolecules* **2007**, *40* (25), 9116−9124.
(57) Li, M.; Fromel, M.; Ranaweera, D.; Rocha, S.; Boyer, C.; Pester, C. W. SI-PET-RAFT: Surface-Initiated Photoinduced Electron Transfer-Reversible Addition-Fragmentation Chain Transfer Polymerization. *ACS Macro Lett.* **2019**, *8* (4), 374−380.
(58) Seo, S. E.; Discekici, E. H.; Zhang, Y.; Bates, C. M.; Hawker, C. J. Surface-Initiated PET-RAFT Polymerization under Metal-Free and Ambient Conditions Using Enzyme Degassing. *J. Polym. Sci.* **2020**, *58* (1), 70−76.
(59) Fromel, M.; Crisci, R. L.; Sankhe, C. S.; Reifsnyder Hickey, D.; Tighe, T. B.; Gomez, E. W.; Pester, C. W. User-Friendly Chemical Patterning with Digital Light Projection Polymer Brush Photolithography. *Eur. Polym. J.* **2021**, *158* (April), No. 110652.
(60) Li, M.; Fromel, M.; Ranaweera, D.; Rocha, S.; Boyer, C.; Pester, C. W. SI-PET-RAFT: Surface-Initiated Photoinduced Electron Transfer-Reversible Addition-Fragmentation Chain Transfer Polymerization. *ACS Macro Lett.* **2019**, *8* (4), 374−380.
(61) Fromel, M.; Sweeder, D. M.; Jang, S.; Williams, T. A.; Kim, S. H.; Pester, C. W. Superhydrophilic Polymer Brushes with High Durability and Anti-Fogging Activity. *ACS Applied Polymer Materials* **2021**, *3* (10), 5291−5301.
(62) Fromel, M.; Pester, C. W. Polycarbonate Surface Modification via Aqueous SI-PET-RAFT. *Macromolecules* **2022**, *55* (12), 4907−4915.
(63) Tsujii, Y.; Ejaz, M.; Sato, K.; Goto, A.; Fukuda, T. Mechanism and Kinetics of RAFT-Mediated Graft Polymerization of Styrene on a Solid Surface. 1. Experimental Evidence of Surface Radical Migration. *Macromolecules* **2001**, *34* (26), 8872−8878.
(64) Xu, J.; Jung, K.; Atme, A.; Shanmugam, S.; Boyer, C. A Robust and Versatile Photoinduced Living Polymerization of Conjugated and Unconjugated Monomers and Its Oxygen Tolerance. *J. Am. Chem. Soc.* **2014**, *136* (14), 5508−5519.
(65) Li, M.; Fromel, M.; Ranaweera, D.; Pester, C. W. Comparison of Long-Term Stability of Initiating Monolayers in Surface-Initiated Controlled Radical Polymerizations. *Macromol. Rapid Commun.* **2020**, *41* (17), 2000337.
(66) Jordan, R.; Ulman, A.; Kang, J. F.; Rafailovich, M. H.; Sokolov, J. Surface-Initiated Anionic Polymerization of Styrene by Means of Self Assembled Monolayers. *J. Am. Chem. Soc.* **1999**, *121* (5), 1016−1022.
(67) Harris, B. P.; Metters, A. T. Generation and Characterization of Photopolymerized Polymer Brush Gradients. *Macromolecules* **2006**, *39* (8), 2764−2772.
(68) Fromel, M.; Li, M.; Pester, C. W. Surface Engineering with Polymer Brush Photolithography. *Macromol. Rapid Commun.* **2020**, *41* (18), 1−17.
(69) Ducker, R.; Garcia, A.; Zhang, J.; Chen, T.; Zauscher, S. Polymeric and Biomacromolecular Brush Nanostructures: Progress in Synthesis, Patterning and Characterization. *Soft Matter* **2008**, *4* (9), 1774−1786.
(70) Fromel, M. Oxygen-Tolerant Photopolymerization for Advanced Functional Surfaces. Ph.D. Dissertation, Pennsylvania State University, University Park, PA, 2022. https://etda.libraries.psu.edu/catalog/20796mef252.
(71) Li, M. Surface modification with polymer brushes via light-mediated polymerization. Ph.D. Dissertation; Pennsylvania State University, University Park, PA, 2022. https://etda.libraries.psu.edu/catalog/23782mul444.

https://doi.org/10.1021/acspolymersau.3c00028
ACS Polym. Au 2023, 3, 428−436